



CHAPTER II

THEORETICAL BACKGROUND AND LITERATURE REVIEW

Fuel cell is the device that converts the chemical energy to electricity. The most used fuels are hydrogen which releases water as a by-product, and methanol where water and carbon dioxide are the by-products. Fuel cells are used in long life batteries which require the continuous fuel and oxygen. Fuel cell was first developed in 1839 by William Grove for the NASA mission. Fuel cell also has other applications such as small vehicle, automobiles, mobile phone, digital camera and laptop.

Varieties of fuel cell are presently used. All of these fuel cells use the same operating principle. Fuel cell system is composed of three components; an anode, a cathode, and an electrolyte which is sandwiched in between. The oxidation and the reduction occur on the interface of these components. The result is that the fuel is consumed and creates water or carbon dioxide. The electricity is generated which creates various electrical applications.

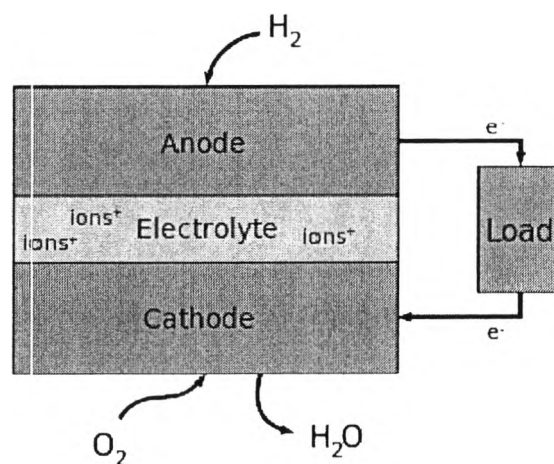


Figure 2.1 Operation principle of hydrogen fuel cell.

The system consists of two electrodes: anode and cathode. The oxidation occurs at the anode side. An anode reacts with the fuel, hydrogen or methanol, and splits it into positive charged ions and the negatively charged electrons. The positive charged ions (protons) travel across the electrolyte to the cathode. The electrolyte is a material that

ions can pass through but electrons cannot. The electrons in turn pass through the wire generating the electric current and then go to the cathode. When positive charged ions and electrons reach cathode, they combine with oxygen and create water or carbon dioxide, a reaction known as the reduction. The reduction occurs at the cathode side. The reaction of the anode and cathode of hydrogen and methanol feeds are shown in table 2.1. The fuel cell is an efficient energy source with zero pollution. In theory, it is possible to get 80 – 90% efficiency from a fuel cell. A good operation generally runs in silence and with a clean waste.

Table 2.1 Reactions of a polymer electrolyte membrane of hydrogen and methanol feeds

Reaction	Hydrogen feed	Methanol feed
At the anode	$H_2 \rightarrow 2H^+ + 2e^-$	$CH_3OH + H_2O \rightarrow 6H^+ + 6e^- + CO_2$
At the cathode	$\frac{1}{2} O_2 + 2H^+ + 2e^- \rightarrow H_2O$	$\frac{1}{2} O_2 + 2H^+ + 2e^- \rightarrow H_2O$
Over all reaction	$H_2 + \frac{1}{2} O_2 \rightarrow H_2O$	$2CH_3OH + 3O_2 \rightarrow 2H_2O + 4CO_2$

2.1 Types of Fuel Cell

There are many types of fuel cell as distinguished by the type of electrode and the operating temperature.

2.1.1 Alkaline Fuel Cell

2.1 Types of Fuel Cell

There are many types of fuel cell as distinguished by the type of electrode and the operating temperature.

2.1.1 Alkaline Fuel Cell

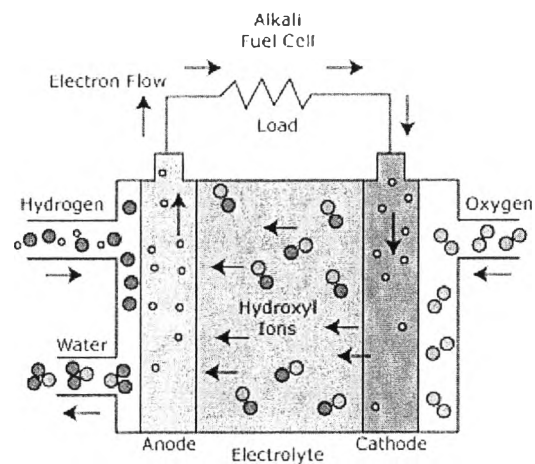


Figure 2.2 Operation of alkaline fuel cell.

Alkaline fuel cells are the simplest type of fuel cell. In an alkaline fuel cell, the system is composed of an anode, a cathode, and an electrolyte in which the electrolyte is the solution of potassium hydroxide in water. Hydrogen reacts with hydroxyl ion at the anode where water and electrons are produced. The generated electrons pass through the external circuit to react with oxygen at the cathode and create hydroxyl ions. The capacity of the cell is limited since it is to operate in a low temperature below 90 °C. The platinum is used as the catalyst to obtain a high power density. The alkaline fuel cell is mostly used in aerospace and military applications. Alkaline fuel cells do not use noble metal as electrocatalysts which are better than acid one. But the challenge to utilize alkaline fuel cell is the removal of carbondioxide in gas stream before entering and depositing into the fuel cell stack (Yeager *et al.*, 1986 and Solomon *et al.*, 1985).

2.1.2 Phosphoric Acid Fuel Cell

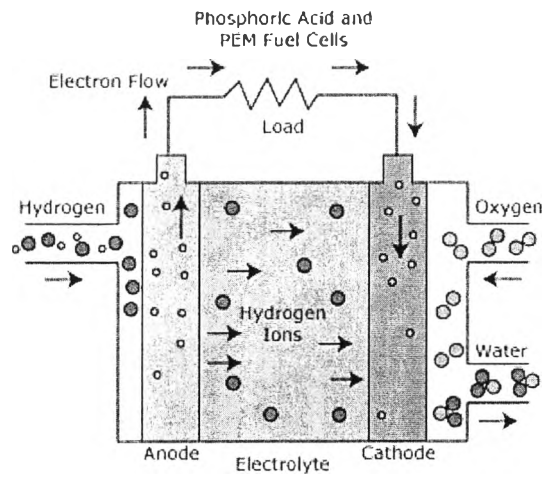


Figure 2.3 Operation principle of phosphoric acid fuel cell.

The phosphoric acid fuel cells have been used since the late 1960s. The principle of phosphoric acid fuel cell is similar to that of a hydrogen fuel cell. The phosphoric acid fuel cell uses a phosphoric acid liquid as an electrolyte. The phosphoric acid fuel cells have good stability and low vapor pressure. Drawback of phosphoric acid fuel cells is that kinetic of oxygen reception occurs in slow rate because of the inhibition of phosphoric absorption. Most phosphoric acid fuel cells operate between 190 – 205 °C, depending on size and applications (Srinivisan *et al.*, 1993).

2.1.3 Solid Oxide Fuel Cell

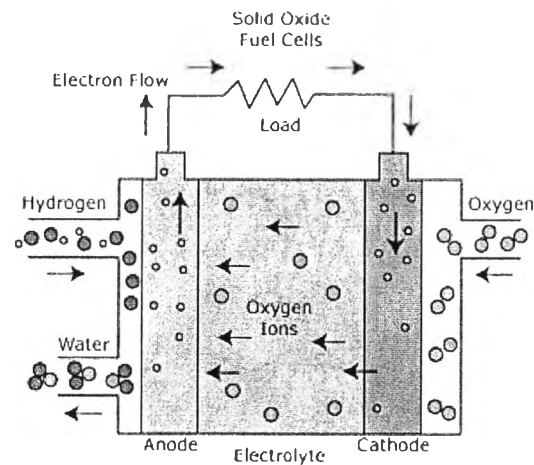


Figure 2.4 Operation of solid oxide fuel cell.

For the solid oxide fuel cell, the hydrogen fuels react with oxide ions to create the water and electrons passing through the external circuit. The electrons reach the cathode and react with oxygen to generate oxide ions migrating through the electrolyte to the anode. The conduction occurs by the diffusion of oxygen ions through the electrode. The system can operate around 1000 °C. The performance has been limited by the thin layer of electrolyte with the conducting oxide and the metallic nickel electrode. The electrolyte of this reaction is zirconia stabilized with yttria. The first type of this fuel cell used in the space application is proton exchange fuel cells using a solid electrolyte made from an ion conducting polymer. The disadvantage of the solid oxide fuel cell is that thermal expansion of cell component which is difficult to control (Tsai *et al.*, 2011).

2.1.4 Molten Carbonated Fuel

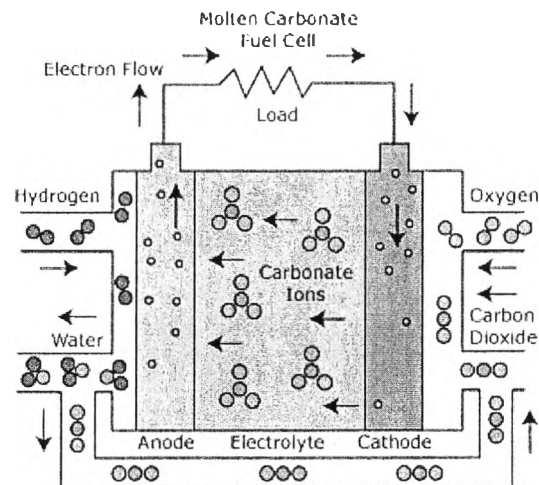


Figure 2.5 Operation of molten carbonate fuel cell.

The molten carbonate fuel cell is a high temperature fuel cell. The hydrogen fuel is feed to the anode to react with carbonated ions. Water and electrons are generated. The electrons flow through an external circuit and go to the cathode. Oxygen and carbondioxide at the cathode react with electrons and create the carbonate ions migrating through the electrolyte. The electrolyte is the mixture of molten carbonate salts in a ceramic matrix. The operating temperature of the molten carbonated fuel cell is around 600 to 700 °C. The disadvantage of the molten carbonated fuel cell is that the corrosive nature of electrolyte (molten alkaline carbonate) which occurs and creates problems at the high temperature operation (Antolini, 2011).

2.1.5 Direct Methanol Fuel Cell

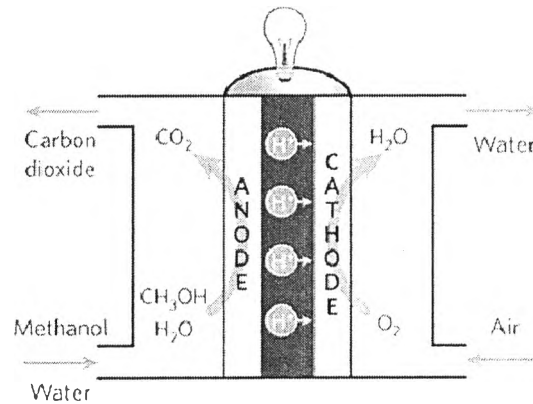


Figure 2.6 Operation of direct methanol fuel cell.

The direct methanol fuel cell is the fuel cells which use the methanol as the fuel. The methanol and water is feed into the system at an anode. Methanol is oxidized at the catalyst layer and creates protons, electrons and carbondioxide; the protons migrate through the electrolyte and electrons flow pass through external circuit to the cathode. Electrons and protons react with the oxygen and create water. The operating temperature of direct methanol fuel cell is in the range 50 to 130 °C which is lower operating temperature than other another types of fuel cell. The direct methanol fuel cell uses a liquid fuel which is easy to recharge. The direct methanol fuel cell still has some disadvantages: methanol crossover and the high cost of commercial electrolyte (Nafion[®]) (Wasmus and Küver, 1999).

2.2 Types of Proton Exchange Membrane

Dupont developed the commercial membrane namely Nafion[®] which consists of perflurosulfonic acid. Nafion[®] has high proton conductivity, good chemical and thermal stability. But high cost and high methanol crossover still limit their application. Many types of the proton exchange membrane were synthesized. The proton exchange membrane should have high proton conductivity to carries the current in the form of proton from one side of electrode to the other side. The membrane should be strong and

moist to prevent conductivity lost. The methanol permeability of the membrane should be low for the direct methanol fuel cell application. One of the effective types of the proton exchange membrane is the sulfonated polymer membrane.

2.2.1 Polysulfones

4,4'-biphenol based disulfonated poly(arylene ether sulfone) copolymers was synthesized as a proton exchange membrane for direct methanol fuel cell by Kima *et al.* (2004). The copolymer was synthesized in two functional morphological regimes; close structure and open structure depending on the degree of sulfonation. 4,4'-biphenol based disulfonated poly(arylene ether sulfone) copolymers had higher selectivity than Nafion[®] due to much lower methanol permeability. When degree of sulfonation increased, the closed structures showed increasing selectivity while the opened structures showed decreasing selectivity.

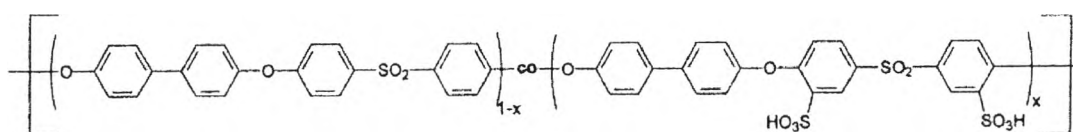


Figure 2.7 The chemical structure of sulfonated poly(arylene ether sulfone).

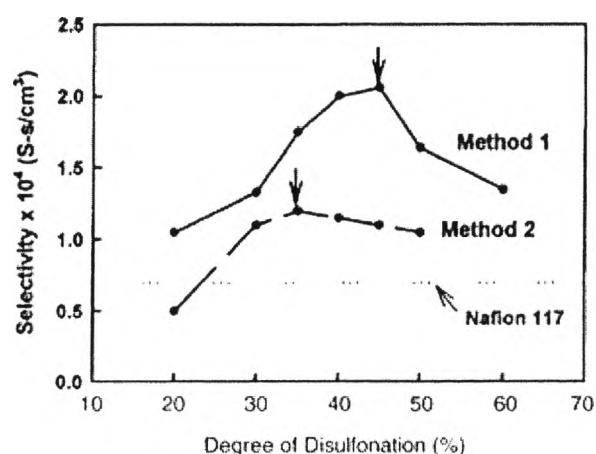


Figure 2.8 Selectivity of 4,4'-biphenol based disulfonated poly(arylene ether sulfone) copolymers and Nafion[®] at 25 °C.

2.2.2 Polyether-Ketones

Sulfonated poly(ether ether ketone) with various degrees of sulfonation was synthesized by Li *et al.* (2003). Sulfonated poly(ether ether ketone) showed high conductivity around 10^{-2} S cm⁻¹ at 80 °C which was close to that of Nafion[®] 115 and methanol permeability of sulfonated poly(ether ether ketone) was lower than Nafion[®] 115.

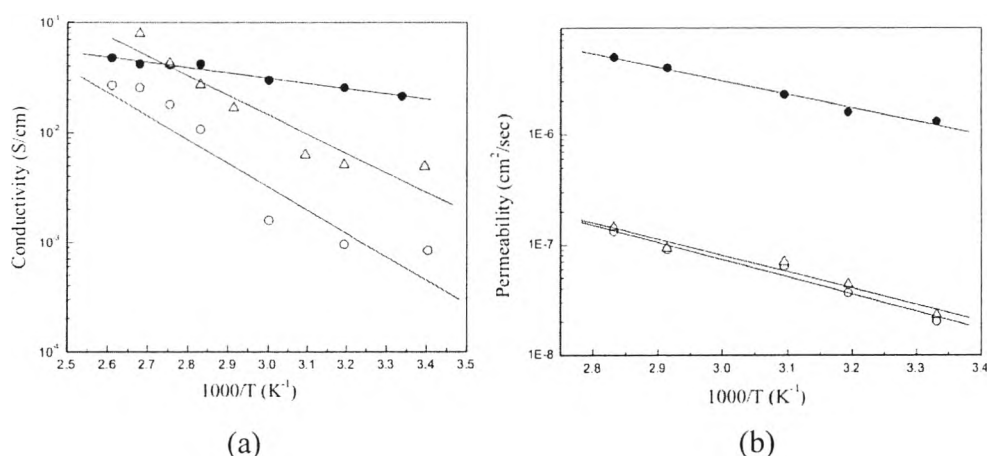


Figure 2.9 Sulfonated poly(ether ether ketone) properties: (a) Arrhenius plots of proton conductivity; and (b) Arrhenius plots of the methanol permeability for samples.

2.2.3 Polybenzimidazoles

Kang *et al.* (2009) synthesized sulfonated polybenzimidazoles with various degree of sulfonation. Sulfonated polybenzimidazoles exhibited distinct properties: transparent, tough, flexible and resistant to high temperature. The morphology of sulfonated polybenzimidazoles was shown taken by TEM displaying larger hydrophilic ionic channels with a higher degree of sulfonation. Water uptake and proton conductivity also increased with increasing degree of sulfonation.

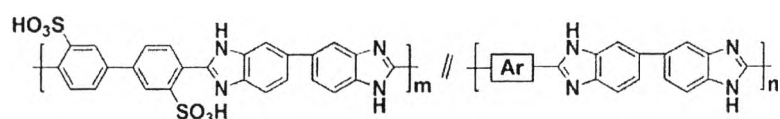


Figure 2.10 The chemical structure of sulfonated polybenzimidazoles.

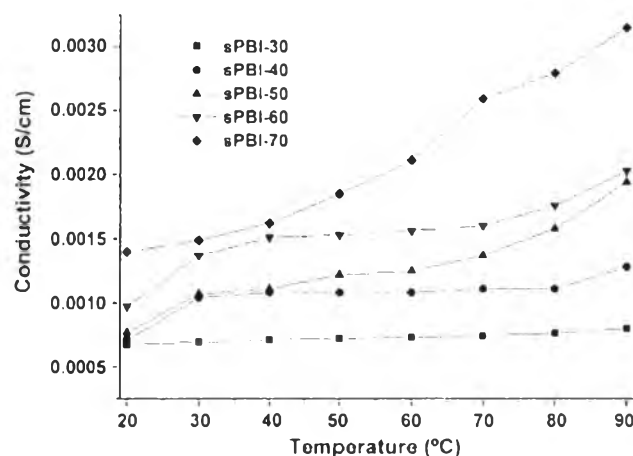


Figure 2.11 Proton conductivity of sulfonated polybenzimidazoles with various temperature.

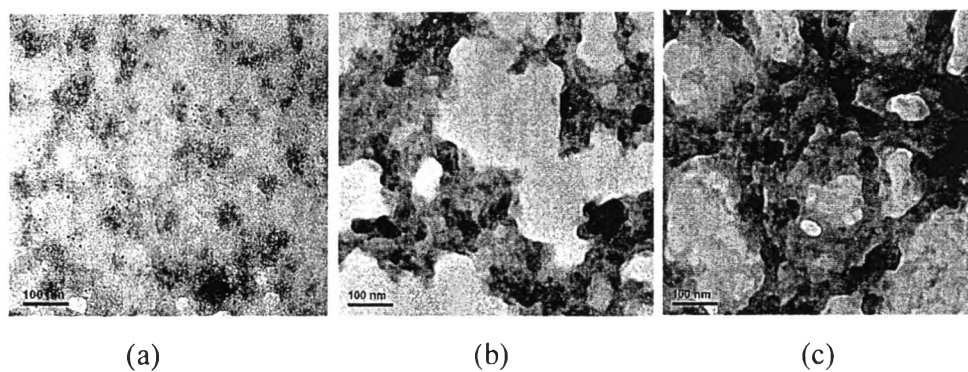


Figure 2.12 TEM image of sulfonated polybenzimidazoles at mole ratio of 3,3'-disulfonate-4,4'-dicarboxylbiphenyl: (a) 30%; (b) 50%; and (c) 70%.

2.2.4 Poly(phenylene oxide)

Proton exchange membrane made from sulfonated poly(phenylene oxide) was synthesized by Liu *et al.* (2007). Sulfonated poly(phenylene oxide) showed high thermal stability. The conductivity of sulfonated poly(phenylene oxide) increased with temperature and the highest proton conductivity ($6.92 \times 10^{-3} \text{ S cm}^{-1}$) was shown at the 2 molar ratio of imidazole to sulfonation poly(phenylene oxide).

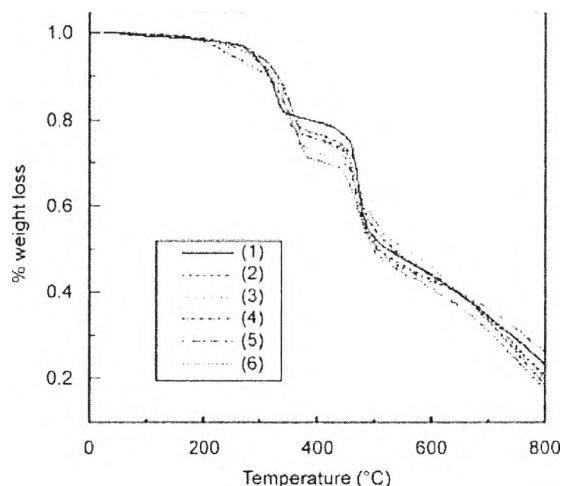


Figure 2.13 The TGA curve of sulfonated poly(phenylene oxide).

2.2.5 Polvimide

Vallejo *et al.* (1999) synthesized a new ion exchange membrane. They used 2,2'-diamino 4,4'-biphenylsulfonic acid, 1,4,5,8-tetracarboxylic acid and another two different sulfonated diamides, and then compared properties with those of the Nafion[®] membrane. The proton transport numbers of both sulfonated polyimide membranes were 10% higher than that of Nafion[®].

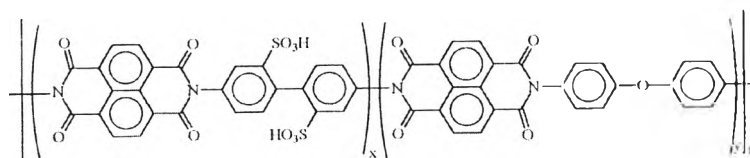


Figure 2.14 The chemical structure of sulfonated polyimide (Vallejo *et al.*, 1999).

Fang *et al.* (2002) studied properties of 4,4'-diaminodiphenyl ether 2,2'-disulfonic acid-based (ODADS-based) and compared properties with those of the sulfonated diamine 2,2'-benzidine disulfonic acid-based (BDSA-based) polyimide membrane. ODADS polyimide displayed greater water stability and better oxidation stability than those of the BDSA polyimide. The synthesized membranes displayed water stability as well as high proton conductivity. The water uptake of polyimide

membranes was not affected by the flexibility of the sulfonated diamine but dependent on various unsulfonated diamines.

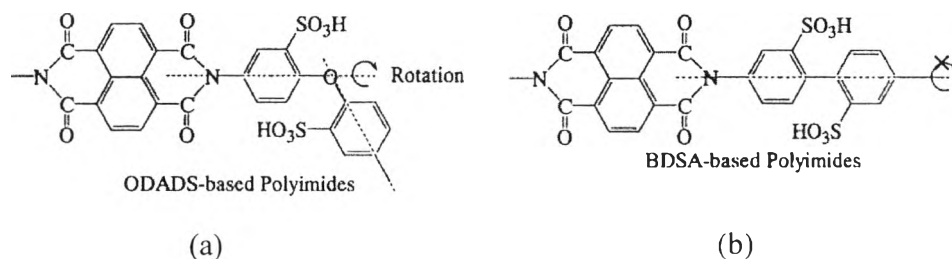


Figure 2.15 The chemical structure of sulfonated polyimide: (a) 4,4'-diaminodiphenyl ether 2,2'-disulfonic acid-based (ODADS-based); and (b) sulfonated diamine 2,2'-benzidine disulfonic acid-based (BDSA-based) polyimide (Fang *et al.*, 2002).

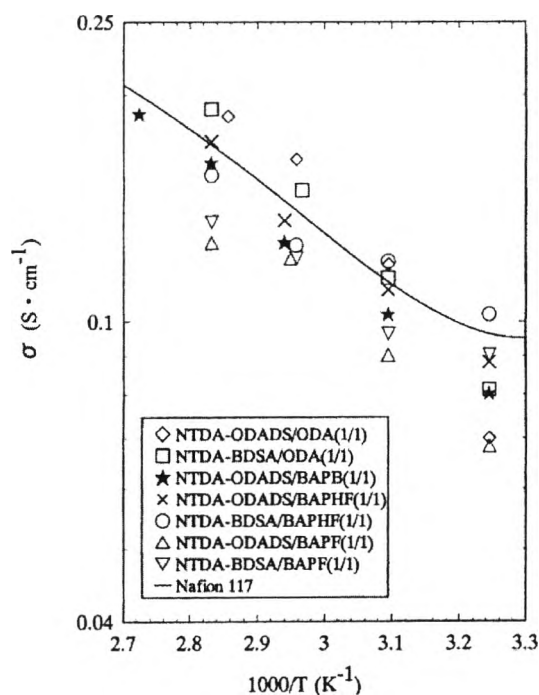


Figure 2.16 The methanol permeability of ODADS-based, BDSA-based and Nafion[®] (Fang *et al.*, 2002).

Woo *et al.* (2003) studied the relationship between the sulfonation level of 2,2'-diamino 4,4'-biphenylsulfonic acid, 3,3',4,4'-benzophenonetetracarboxylic dianhydride and a unsulfonated diamine. FTIR was used to investigate the structure.

They found that when increasing the sulfonation level up to 30-35 mol%, the proton conductivity, the methanol permeability, and the amount of water uptake were increased. The synthesized sulfonated polyimide membrane exhibited thermal stability up to 300 °C and absorbed five times less water than Nafion[®].

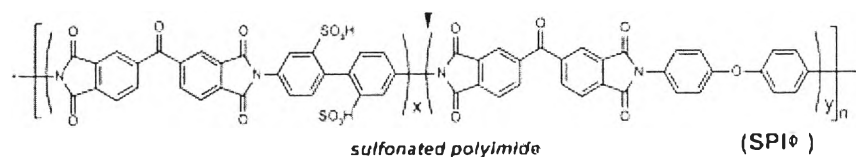


Figure 2.17 The chemical structure of sulfonated copolyimide (Woo *et al.*, 2003).

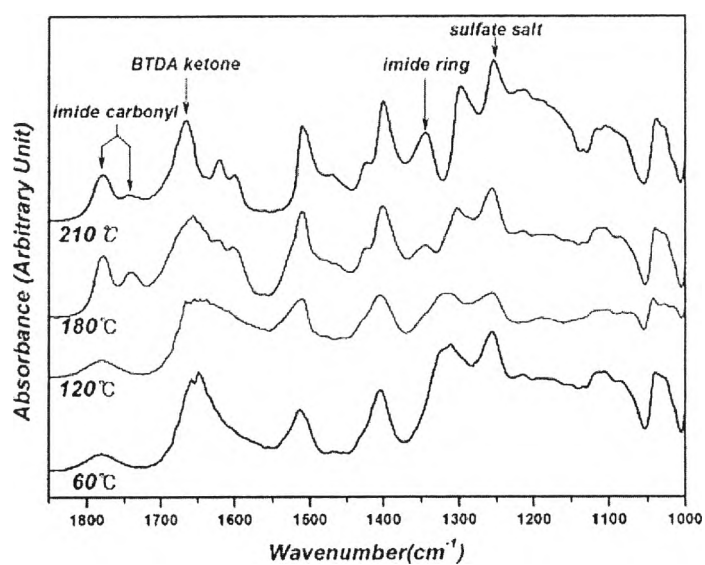


Figure 2.18 The FTIR spectra of sulfonated copolyimide (Woo *et al.*, 2003).

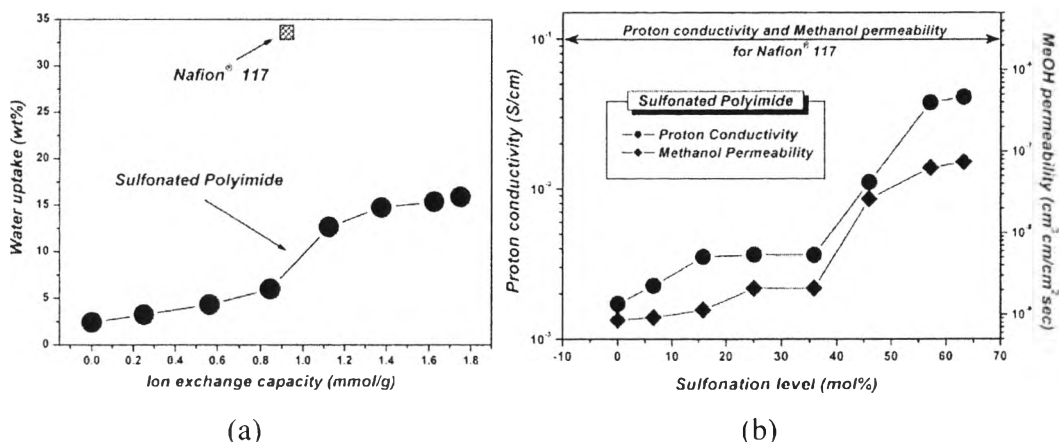


Figure 2.19 (a) Water uptake as a function of ion exchange capacity of sulfonated polyimide; and (b) Proton conductivity and methanol permeability as a function of sulfonation level (Woo *et al.*, 2003).

Blázquez *et al.* (2005) studied the effect of solvent and the acidification method on the membrane properties. The water vapor sorption depended on the acidification, the solvent, and the ion exchange capacity (IEC). The density of membrane was high for the acidification with an ion interchange resin in a solution while the acidification with 0.1 M H₂SO₄ at an ambient temperature was at a better performance in the fuel cell test. Types of solvent affected the proton conductivity of the membrane. NMP solvent slightly enhanced the membrane proton conductivity. The proton conductivity increased with IEC, for 2.3 meqH⁺q⁻¹, and at a temperature higher than 40 °C the membrane was soluble in water.

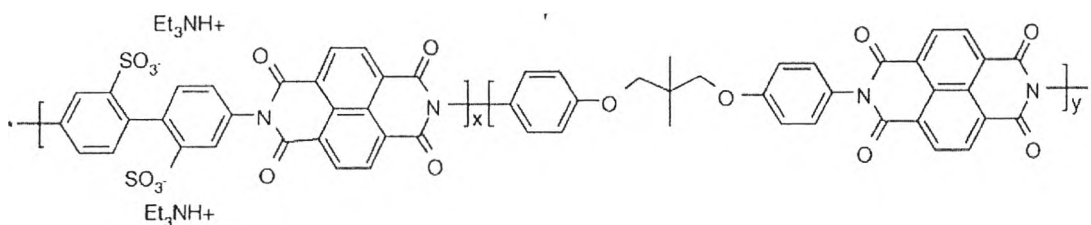


Figure 2.20 The chemical structure of sulfonated naphthalenic polyimides (Blázquez *et al.*, 2005).

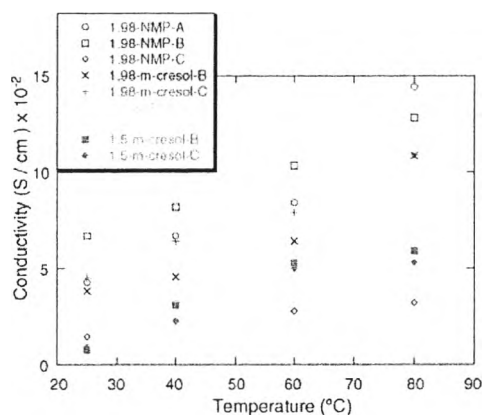


Figure 2.21 Temperature dependence of conductivity of the membrane with different type of solvent (Blázquez *et al.*, 2005).

Sulfonated copolyimides using 4,4'-bis(4-aminophenoxy)benzophenone-3,3'-disulfonic acid (BAPBPDS) and 4,4'-bis(4-aminophenylthio)benzophenone-3,3'-disulfonic acid (BAPTBPDS) were synthesized. 1,4,5,8-naphthalenetetracarboxylic dianhydride were used as the main monomer. TGA curve of sulfonated copolyimide displayed the decomposition of sulfonic group around 300 °C and the decomposition of polymer main chain around 500 °C. Zhai *et al.* (2007) found that the sulfonated polyimide membrane with the aromatic structure displayed good thermal stability, high mechanical strength and modulus, greater electrical property, good chemical resistance and low methanol permeability. The higher basicity of BAPTBPDS in membrane displayed higher water stability and higher proton conductivity.

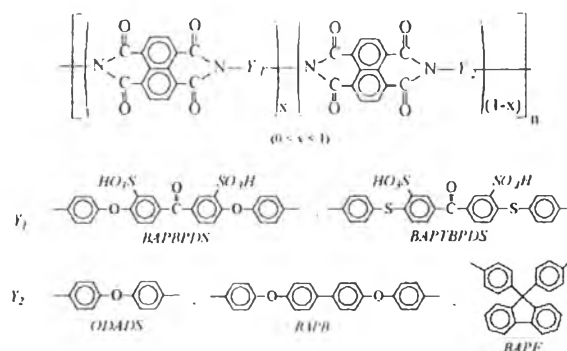


Figure 2.22 The chemical structure of sulfonated polyimides (Zhai *et al.*, 2007).

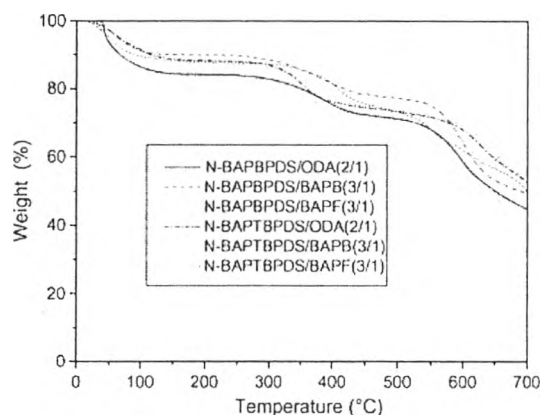


Figure 2.23 The TGA curve of sulfonated polyimides (Zhai *et al.*, 2007).

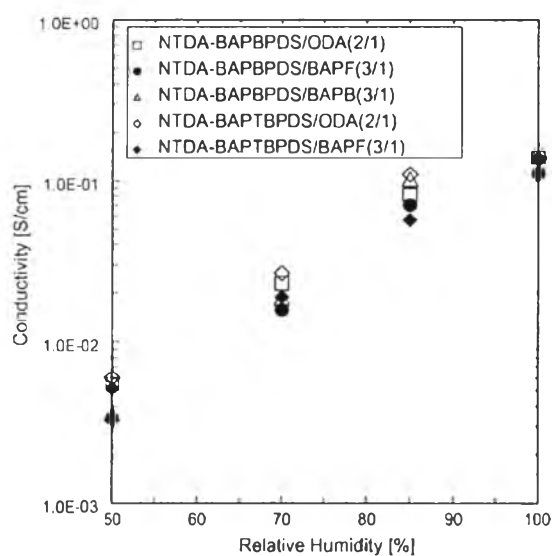


Figure 2.24 Relative humidity dependence of conductivity of the membrane with different type of monomer (Zhai *et al.*, 2007).

Li *et al.* (2007) synthesized a polyimide membrane from 3,3',4,4'-benzophenonetetra-carboxylic dianhydride, 4,4'-diaminodiphenylmethane and 4,4'-oxydianiline with two different methods: one was the microwave-assisted polycondensation; and another one was the conventional solution polycondensation microwave assisted polycondensation. The former method gave a higher yield and viscosity at the same reaction condition and reaction time.

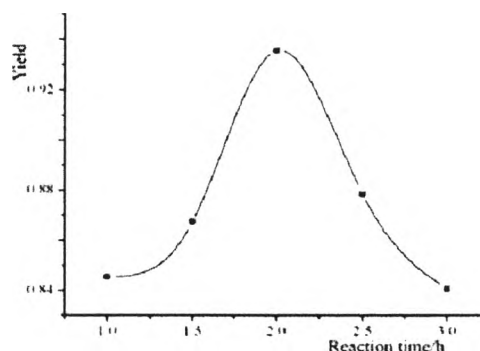


Figure 2.25 Effect of the microwave irradiation time on the yield of polyimide (Li *et al.*, 2007).

Matsuguchi *et al.* (2006) synthesized a semi-IPN membrane composed of Nafion[®] and cross-linked divinylbenzene. The cast film exhibited a low swelling ratio and low methanol permeability but also with reduced proton conductivity. The conductivity of divinylbenzene/Nafion[®] = 0.06 at 30 °C and 80% relative humidity was 4.5×10^{-3} S/cm which was lower than that of the unmodified Nafion[®]. The absence of ion cluster was the main cause of the low proton conductivity.

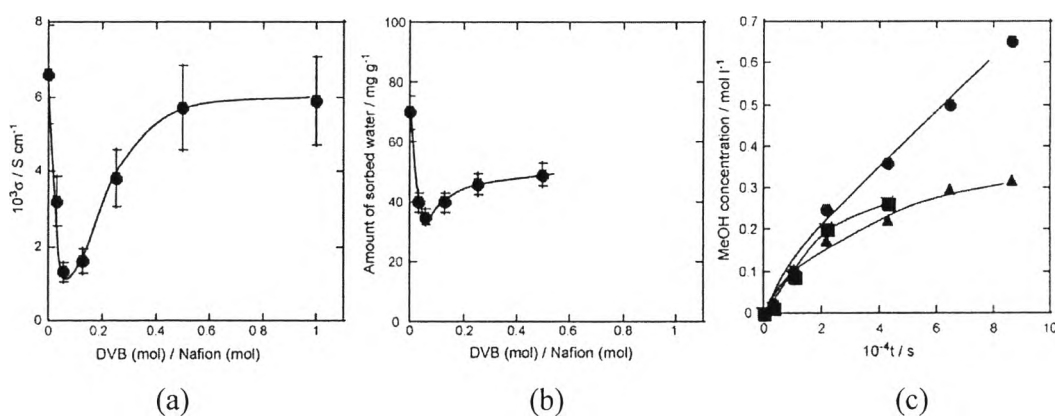


Figure 2.26 The properties of sulfonated polyimide: (a) proton conductivity at 30 °C and 80% RH; (b) amount of adsorbed water at 30 °C and 50% RH as a function of DVB composition in semi-IPN coating films measured; and (c) methanol concentration during permeation test (Matsuguchi *et al.*, 2006).

Okamoto *et al.* (2005) prepared two types of sulfonated co-polyimides from 1,4,5,8-naphthalenetetracarboxylic dianhydride which reacted with 4,4'-bis(4-sulfophenoxy)biphenyl-3,3'-disulfonic acid or reacted with bis(3-sulfopropoxy)benzidines and a common non-sulfonated diamine. These two types of sulfonated co-polyimides exhibited the conductivity similar to that of Nafion[®] 112 in water at 323 K. The methanol permeability of sulfonated co-polyimides was more than two times lower than the value of Nafion[®] 112.

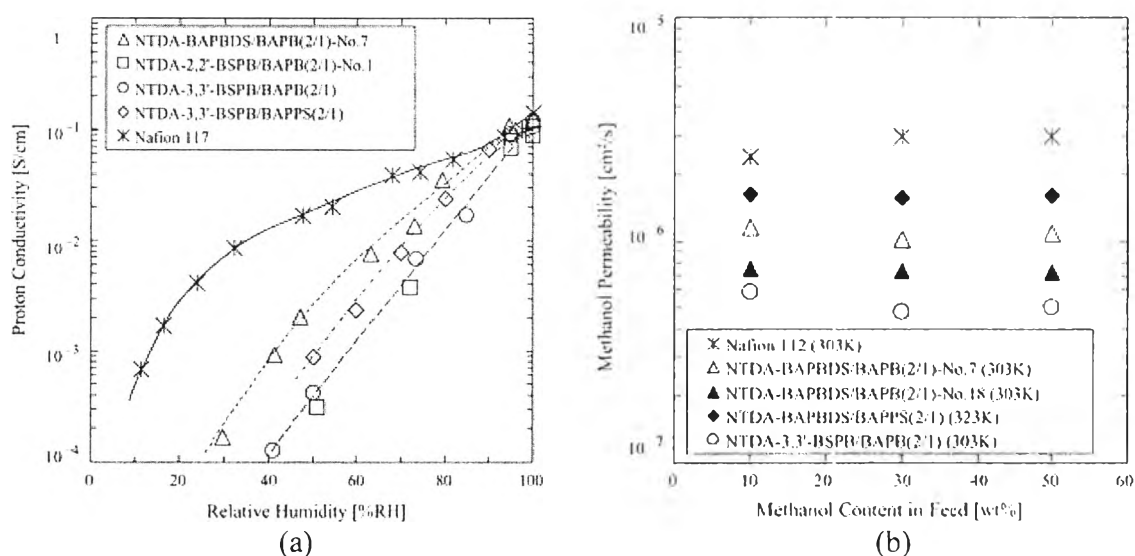


Figure 2.27 The properties of sulfonated polyimide: (a) proton conductivity; and (b) methanol permeability (Okamoto *et al.*, 2005).

In 2008, Li *et al.* synthesized a novel sulfonated poly(arylene-co-imide)s with have $-SO_3$ on the side chain. The polyimide was obtained from sodium 3-(2,5-dichlorobenzoyl)benzenesulfonate and naphthalimide dichloride monomer. DMA was used to investigate mechanical properties. The membrane displayed toughness and flexibility and exhibited water stability. The proton conductivity of copolymer increased with increasing ion exchange capacity and temperature.

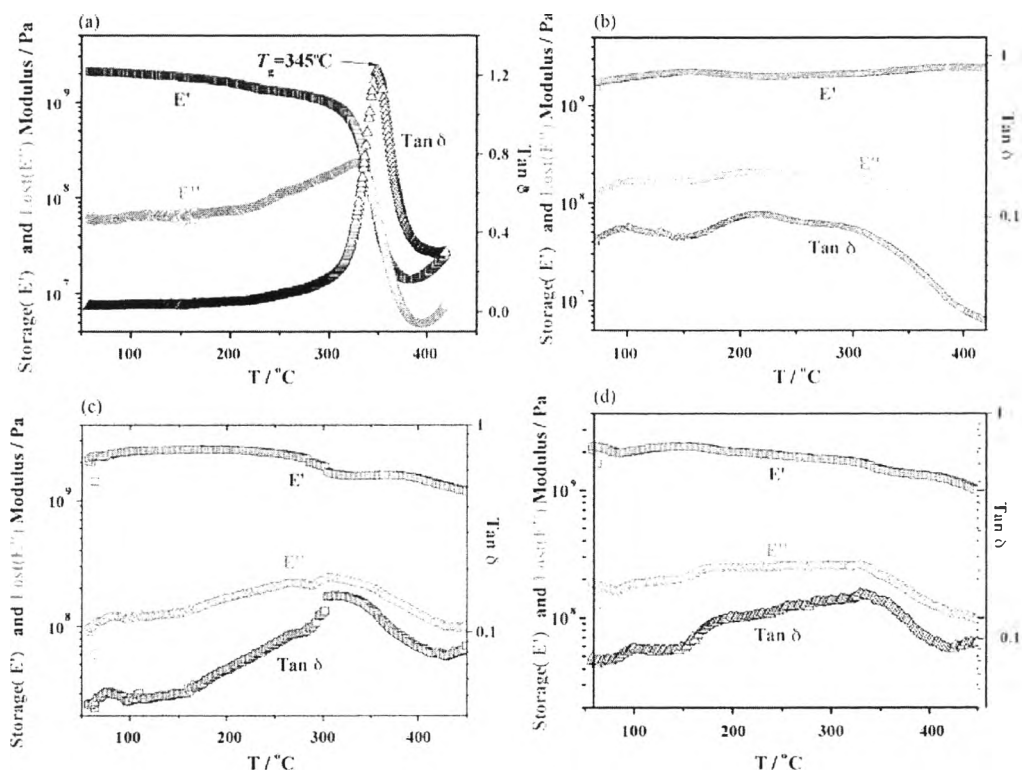


Figure 2.28 The dynamic mechanical behavior of sulfonated poly(arylene-co-imide)s (Li *et al.*, 2008).

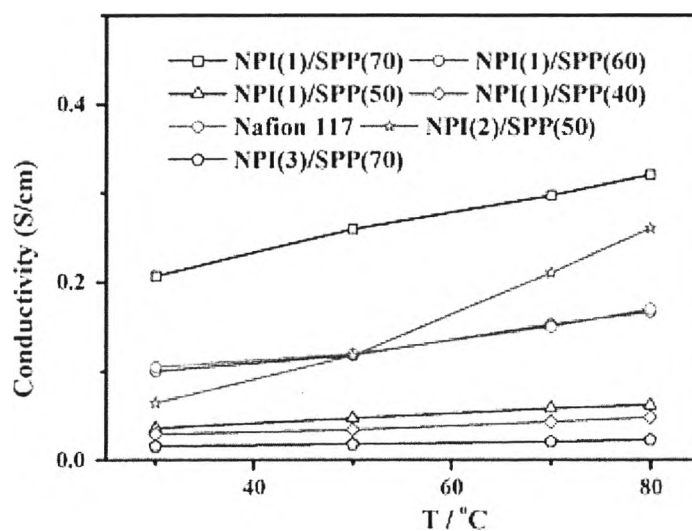


Figure 2.29 The conductivity of sulfonated poly(arylene-co-imide)s (Li *et al.*, 2008).